SKI Report 2003:33

Research

Characterization of the Microstructure in Recrystallized Zircaloy-2 Cladding Irradiated to a High Neutron Dose

Kjell Pettersson

April 2003

ISSN 1104–1374
ISRN SKI-R-03/33-SE

SKI-perspektiv

Bakgrund

Då bränslestavarna bränns ut i härden på kärnkraftsreaktorerna utsätts stavarnas kapslingsmaterial för en neutronbestrålning som leder till stora förändringar i materialet. Materialet hårdnar samtidigt som det blir mindre tåligt för att deformeras. De små så kallade sekundärfaspartiklar som finns i materialet och som anses ha stor betydelse för materialets korrosionsegenskaper amorfiseras och börjar lösas upp. 2001 uttryckte den japanska organisationen Criepi ett intresse för att med hjälp av elektronmikroskopi karakterisera mikrostrukturen i kapslingsmaterial, som bestrålats ovanligt lång tid, 12 år, i Ringhals 1. Bakgrunden till deras intresse var ett antal som de ansåg oförklarliga bränsleskador i Japan vilka eventuellt skulle kunna få sin förklaring genom en strukturstudie. Studierna skulle utföras med deras egen personal.

SKI:s syfte

För att vidmakthålla den kompetens som finns i Sverige avseende denna typ av studier, samt för att få snabb information utifall de japanska skadorna var ett nytt tidigare okänt fenomen, beslöt SKI att en av japanerna oberoende karakterserings-arbete skulle göras av svenska forskare.

Resultat

Denna studie redovisas i föreliggande rapport som visar att mikrostrukturen i Ringhalsmaterialet i allt väsentligt överensstämmer med vad som observerats tidigare på Zircaloy som bestrålats till hög neutrondos. Det har sedermera framkommit att de japanska bränsleskadorna med stor sannolikhet orsakats av väteinducerat fördröjt brott, ett fenomen där SKI tidigare stött en relativt omfattande forskning.

Projektinformation

SKI:s projekthandläggare: Jan in de Betou
SKI:s projektnummer: 01257

SKI Report 2003:33

Research

Characterization of the Microstructure in Recrystallized Zircaloy-2 Cladding Irradiated to a High Neutron Dose

Kjell Pettersson

MATSAFE AB
Att: Kjell Pettersson
Skeppargatan 84, bv
114 59 Stockholm

April 2003

Table of contents

Characterization of the microstructure in recrystallized Zircaloy-2 cladding irradiated to a high neutron dose. SKI-project 14.6-011209:01257.

Kjell Pettersson
Matsafe AB.

Summary

The objectives of the present project were to determine if there is anything in the microstructure of highly irradiated Zircaloy-2 which may make the material fracture in a brittle manner. Samples were taken from three different locations on a fuel rod which had been irradiated for 12 years. The displacement doses were estimated to be 1.4, 9 and 28 dpa. Specimens for electron microscopy were prepared with two different orientation called axial and radial. In the axial orientation the electron beam goes parallel with the basal plane and diffraction conditions can be arranged so that dislocations with **a** Burgers' vectors become invisible. In the low dose specimen only **a** component damage was present and all second phase particles were crystalline. In both the high and intermediate dose samples there was **c** component damage present with a slightly higher amount in the high dose sample. The particles of the $Zr(Cr,Fe)_2$ type were generally amorphous in these samples and the Fe-content of the particles was highly redused. The hydride structures were similar in all samples. The hydrides were often precipitated in parallel in the same grain and chains of hydrides were seen which ran from grain to grain. No population of small hydrides were observed except from surface hydrides formed during specimen preparation. It was concluded from the investigation that there is nothing in the microstructure which may make the material in the high dose state subject to a purely mechanically induced fast brittle cracking.

Karakterisering av bestrålningsinducerad mikrostruktur i Zircaloy-2 bestrålad till hög dos.

Kjell Pettersson
Matsafe AB

Sammanfattning.

Motivet för denna undersökning var att bestämma om det finns något i mikrostrukturen i högt bestrålad Zircaloy som gör materialet känsligt för snabba sprödbrott. Prover togs ut från tre olika positioner på en bränslestav som bestrålats i tolv år. Ståldoserna uppskattas till 1.4, 9 och 28 dpa. Prover för elektronmikroskopi preparerades med två skilda orienteringar, axiell och radiell. I den axiella orienteringen går elektronstrålen parallellt med basplanen och man kan arrangera diffraktionsförhållandena så att dislokationer med en **a** Burgers vektor blir osynliga. I materialet med den lägsta stråldosen fanns endast strålskada med **a**-karaktär och alla sekundärfaspartiklar var kristallina. I både det hög- och medelbestrålade materialet fanns strålskada med **c**-karaktär, något mer i det högst bestrålade materialet. Partiklarna av $Zr(Cr,Fe)_2$-typ var i allmänhet amorfiserade och hade förlorat det mesta av sitt järninnehåll. Hydridstrukturerna var likartade i alla proven. Flera hydridskivor skiljs ofta ut parallellt i samma korn. Man ser ofta långa hydridkedjor som går från korn till korn. Det fanns ingen population av små hydrider annat än ythydrider som bildas i samband med provprepareingen. Slutsatsen av undersökningen är att det inte finns något i mikrostrukturen som kan tänkas göra materialet känsligt för ett snabbt sprött brott.

1. Introduction

When zirconium alloys, or any metal for that matter, are irradiated with energetic particles various types of radiation damage may be formed. Due to the use of zirconium alloys in reactors, radiation damage by energetic neutrons is of particular engineering significance. The primary damage event when a neutron strikes a zirconium atom is that a part of the neutron energy is transferred to the zirconium atom. For energetic neutrons, with energies above about 1 keV, the knocked out atom can in turn knock out other atoms from their normal lattice positions. In the core of a reactor there is a large number of neutrons with energies above 1 MeV. When such a neutron hits an atom a large number of atoms,several hundreds, are displaced from their normal lattice positions in a so called displacement cascade [1]. Each displaced atom takes up an interstitial position between the normal lattice sites, and it is consequently called an interstitial, or a self-interstitial, to allow for the fact that sometimes alloy atoms may take up interstitial positions. The vacant site left by a knocked out atom is simply called a vacancy. If an interstitial comes close to a vacant site it is obviously energetically favourable for it to return to this site. This is called recombination. Already in the displacement cascade the majority of defects recombine and when the cascade event is finished perhaps only 5% of the defects remain.

The remaining defects diffuse around in the material and may form defect clusters of vacancies or interstitials. It has long been speculated that vacancy dislocation loops may form directly in the collision cascade by a collapse of the cascade. In a recent review of point defects and clusters in hexagonal metals Bacon [2] cites several experimentally verified examples of cascade collapse with the formation of a vacancy loop in hcp metals. It is also interesting to note that in molecular dynamics simulations of collision cascades not only vacancy loops have been observed but also interstitial loops [3]. However it should be noted that cascade collapse is not a pre-requisite for formation of loops. If there is a supersaturation of interstitials and/or vacancies in the lattice, clusters in the form of loops nucleate and grow quite readily as evidenced for example by the formation of loops by electron irradiation where single Frenkel defect pairs are formed [4]. It may be noted of course that another form of clustering of vacancies is the nucleation and growth of voids. However so far, even though voids have been observed in zirconium alloys, they do not grow in numbers large enough to be of any engineering significance.

Before going into details about observed damage types in zirconium alloys it is perhaps appropriate to present the crystal structure with the most important lattice vectors. A crystal model is shown in Figure 1.

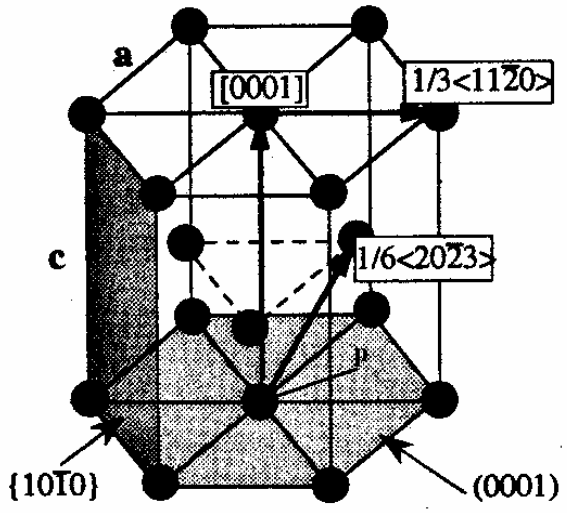

Figure 1. Illustration of the zirconium unit cell and some principal directions and planes.

The hexagonal structure is built up of close-packed planes in the stacking sequence ABABAB….. This has some significance for formation of vacancy loops on the basal planes. If a disc of atoms is removed on the basal plane, atoms in A positions face each other, and a direct collapse is not energetically favourable with regard to bond energies. Therefore loops tend to form with a sideways motion along the vector **p** in the Figure in addition to the collapse **c**/2. Compared to the **c**/2 loop this loop has a higher elastic energy due to its larger Burgers vector, **c/2+p** = $1/6 < 20\bar{2}3 >$, but a lower stacking fault energy since it is still a close-packed structure, a local fcc lattice at the fault. In fact, both types of loops have been observed [4].

The devolopment of the irradiation induced microstructure in zirconium alloys has been investigated since about 1960 in order to improve the understanding of how properties depend on neutron irradiation. In broad terms the major property changes are that the yield strength increases and the uniform elongation decreases with neutron irradiation. These property changes tend to saturate at a relatively low dose of the order of 10^{21} n/cm^2 (E>1MeV) or just a little more than a dpa (displacements per atom). Technologically more important is that on-going neutron irradiation induces or accelerates creep deformation at stress levels and/or temperatures where there is no thermal creep. Another technologically important phenomenon is irradiation growth. In

a cladding tube growth results in an elongation in the axial direction. More generally irradiation growth in zirconium components is characterized by an extension along a direction perpendicular to the c-axis and shrinkage along the c-axis.

The early investigations of the irradiation induced microstructure quite naturally were done on materials with a relatively low neutron dose. At those low doses the microstructure is characterized by a high density of loops with an **a** Burgers' vector. An interesting question is whether these loops have vacancy or interstitial character. For materials irradiated at light water reactor operating temperatures, 280-350 °C the loops are unfortunately too small to permit a determination of their character. However if materials are irradiated at higher temperature or if pure unalloyed zirconium is irradiated at around 300 °C much larger loops are formed for which a character determination is possible. Such determinations were reported as a round-robin exercise in 1979, [5], and they showed that the loops were a mixture of vacancy and interstitial loops, with slightly more vacancy than interstitial loops. Post-irradiation annealing experiments performed in order to grow the smaller loops indicate that those are also to a significant fraction of vacancy character. By that time no loops with **c** component Burgers' vector had been found in neutron irradiated material. It had however been observed in electron irradiated material.

The absence of **c** component damage made the growth phenomenon somewhat of a mystery. Growth is intimately related to the anisotropy of zirconium alloys and zirconium alloy components. As is obvious from Figure 1 a zirconium single crystal must be anisotropic. As other hexagonal metals with c/a < 1.633, the ideal value for a solid-ball hexagonal stacking, zirconium preferentially deforms by glide in the **a** direction on the $<10\bar{1}0>$ prism planes. Other slip systems as well as a number of twinning systems are available but reqiure a much higher stress. As a result of this anisotropy zirconium alloy components manufactured with processes involving plastic deformation will have a pronounced texture, the grains of the material will have a preferred orientation. For a cladding tube a typical texture would be characterized by all basal poles lying in a plane perpendicular to the axial direction. One example of such a texture is that of recrystallized cladding used in Swedish reactors which have a texture with two strong basal pole maxima at ±30 from the radial direction. A very natural explanation why such a tube grows in the axial direction would be to assume that all the **a** loops have interstitial character and that vacancy loops form on the basal plane. However, already in 1976 Northwood [6] showed that the density of **a** loops was not

high enough to explain observed growth strains even if they all had interstitial character, which, as we have seen, they have not.

In the beginning of the eighties the first reports on c-component damage in highly irradiated Zircaloy were published [7]. It was of particular interest that the appearance of the c component damage coincided with the irradiation dose when recrystallized Zircaloy starts to grow at a high rate. In contrast to cold worked Zircaloy which grows with a constant rate from the beginning of irradiation, recrystallized Zircaloy has a transient initial growth which ends with a very low constant growth rate which goes on until a dose of about $5x10^{21}$ n/cm^2 when growth starts to accelerate until a growth rate of the same magnitude as the rate for cold worked material is attained. The c component damage is mainly seen as dislocation segments oriented parallel to the basal planes and we will show examples later in this paper. Only rarely the damage is seen as loops although it is assumed that it starts forming as vacancy loops on the basal plane. A number of subsequent papers confirmed this initial observation [8-12]. A first review on the subject was published by Griffiths in 1988 [4]. In the review Griffiths describes the various forms of c component damage. The most common is the $1/6 < 20\bar{2}3 >$ loop which is invariably vacancy in nature. Other types are the **c**/2 type and the **c**+**a** $=1/3 < 11\bar{2}3 >$.The former is usually of vacancy character and the latter of interstitial character.

The start of formation of c component damage and the break-away growth is associated with the irradiation induced dissolution of second phase particles in zirconium alloys. In Zircaloy-2 for instance the main second phase particles are $Zr(Cr, Fe)_2$ and $Zr_2(Ni, Fe)$. It is observed that **c** component damage starts to form around $Zr(Cr, Fe)_2$ particles when they start to dissolve. For this type of particle the dissolution is also associated with an amorphization of the crystal [9, 13, 14]. Analyses of the particle composition shows that the dissolution starts with Fe leaving the particle. It is believed that Fe moves interstitially in Zr and that its diffusion is fast. However it is probably not the dissolved Fe which promotes the nucleation and growth of **c** component damage but rather the Cr which escapes into the matrix as discussed by Griffiths et. al. [15]. That Fe has no such effect has been demonstrated in Russian work where the microstructural development and growth has been studied in Zr-1Nb and Zr-1.2Sn-1Nb-0.4Fe [16-18]. In the former alloy the main precipitate is β-Nb while the latter contains the Laves phase $Zr(Nb;Fe)_2$. Despite the fact that the latter type of particle goes into solution it is only in the former alloy that significant amounts of **c** component damage is observed. On the other hand de

Carlan et. al. have in a direct study of the influence of Fe on the nucleation of **c** component loops concluded that Fe indeed has an effect on loop nucleation.[17].

The extensive work on characterization of zirconium alloy microstructures were again reviewed in 1995 [19] and the growth characteristics of zirconium alloys were reassessed and it was suggested that growth was slightly non-linear, and accelerating with dose, rather than linear as usually assumed previously [20].

The main concern behind the previous microstructural characterizations has been irradiation growth and cladding corrosion properties and their dependence on precipitate stability. However recently there is some renewed concern about the mechanical integrity of irradiated Zircaloy. A few low-ductile failures have occurred which can not be explained by stress corrosion cracking which previously has been the main cause of low-dultile failures. The present study was undertaken with the objective to determine if there is anything in the irradiation induced microstructure which might explain such low-ductile failures of irradiated Zircaloy cladding. Such studies have been performed previously, notably by Chung and co-workers. Already in 1985 [21] Chung reported a TEM (transmission electron microscope) and SEM (scanning electron microscope) examination of low ductile failures of spent fuel cladding tested by internal pressure or by internal mandrel expansion. In the microstructure Chung identified precipitates of Zr_3O and cubic ZrO_2. The Zr_3O precipitates decorated dislocations and it may be assumed that they were a strong impediment to dislocation motion and thus promoting brittle failure. Also the precipitates of cubic ZrO_2 would contribute to the resistance to plastic deformation. Obviously neither of Zr_3O or ZrO_2 would normally be stable in a Zr matrix. However Chung explained their presence as caused by non-equilibrium segregation effects induced by the irradiation. To the knowledge of the present author Chung's observations have not been corroberated independently.

At the time of Chung's publication delayed hydride cracking (DHC) in the form studied by for instance Efsing or Edsinger had not been identified as a failure mode for irradiated fuel cladding. On inspection of Chung's SEM pictures there is a reasonable similarity with fracture surfaces presented by Efsing [22] and Edsinger [23] so it seems quite conceivavble that Chung's failures are cases of DHC. This is also consistent with the long failure times in the tests where Chung observed the low-ductile failures.

More recently Chung has published two papers addressing the issue of low-ductile failures of irradiated Zircaloy in connection with Reactivity Initiated Accident tests.

One of the papers is concerned with characterization of hydride structures in spent-fuel cladding [24]. Somewhat surprisingly it appears as if nobody before Chung has determined the habit planes of the hydride plates in irradiated cladding. It turns out that in unstressed cladding the habit plane is $\{10\bar{1}7\}$ just as it commonly is in unirradiated material, a fact that has been known for about thirty years [25]. In stressed cladding Chung observes $\{10\bar{1}4\}$ for a tangential stress except for radial hydrides which have a habit plane of $\{10\bar{1}1\}$. In the other report where Chung analyzes the factors behind axial split failures [26] he suggests that one of the main factors behind these failures is family of small δ hydrides which precipitate in highly irradiated material. Obviously, in the present work we have been looking for such features.

2. Experimental details

2.1. Material

The material examined in the present work came from a Zircaloy-2 clad fuel rod which had been irradiated in the Ringhals 1 boiling water reactor for a period of 12 years. Despite this long exposure time no unusual amounts of hydrides have been observed in the post-irradiation examination which was performed in the hot cells in Studsvik. Metallographic cross sections contain the normal stringers of tangentially oriented hydrides [27]. The cladding material, fully recrystallized Zircaloy-2, was manufactured in 1980 to the ASEA-ATOM LK0 specification which means that it originally contained second phase particles of a size typical of cladding where there is no beta quenching late in the process. The cladding diameter was 12,25 mm and the wall thickness 0.8 mm.

As part of the post-irradiation examination of the rod an attempt was made to estimate the fast-neutron dose of the rod from the ^{54}Mn gamma activity of the plenum spring [27]. This resulted in an estimated dose of $3x10^{20}$ n/cm^2 (E>1MeV) in the plenum where one of the cladding samples, the ”plenum sample”, was taken. Just under the plenum where the second sample for the present examination was taken, the ”low burnup sample”, the dose was estimated to be $2x10^{21}$ n/cm^2. The third sample, the ”high burnup sample”, was taken at the 3 m level of the rod where Studsvik estimated that the neutron dose was three times higher, or $6x10^{21}$ n/cm^2.

In the period 1985-1990 structural material tension specimens were irradiated in detector positions in the core of the Barsebäck 1 reactor which is of the same design as the Ringhals 1 reactor, although smaller. From available flux profiles from that experiment it can be expected that the flux on the 3 m level should be about 4-$6x10^{13}$

$n/cm^2/s$. If we take $5x10^{13}$ as a representative value and assume an irradiation time of 8000 hours/year we arrive at a value of $1.6x10^{22}$ n/cm^2 for the high burnup sample. This value is based on an irradiation time of 11 years. In the last year of irradiation the rod was in a peripheral position with a very low flux. This neutron dose corresponds to about 28 dpa. We regard this as a more likely value than the estimate from the ^{54}Mn activity measurement done is Studsvik.

2.2. Specimen preparation.

Short lengths of tube were cut and specimens for TEM examination were extracted in two different orientations, Figure 2. The reason for using two different orientations is that for cladding tubes with the ±30° texture it is impractical if not impossible to tilt a radial specimen so that the electron beam becomes parallel to the basal plane and which is necessary in order to activate the (0002) diffraction. The (0002) diffraction must be activated in order to make dislocations with an **a** Burgers' vector invisible according to the $\mathbf{b}\cdot\mathbf{g} = 0$ criterion. It is normally only when the **a** dislocations are invisible that **c** component dislocations can be identified.

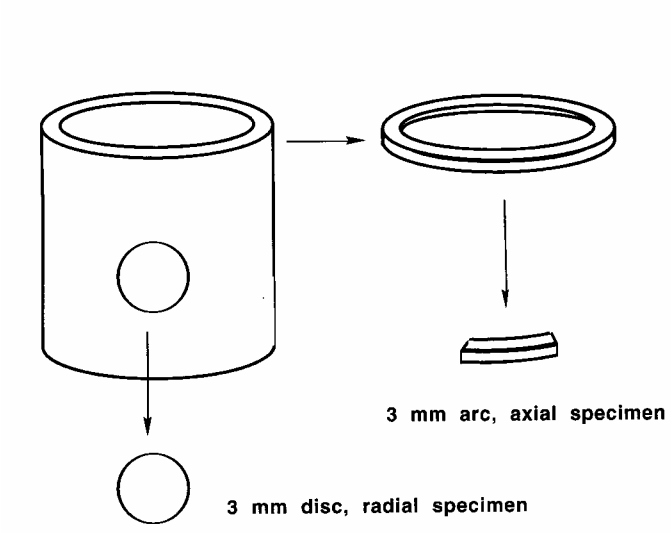

Figure 2. Specimens extracted in two different orientations. The designations "axial" and "radial" refers to the direction of the electron beam on examination of an untilted specimen in the TEM.

The preparation of radial specimens was done by extracting a square piece of clad wall and grinding it to a thickness of about 0.1 mm. The grinding also removed the curvature so from the flat piece that was left a 3 mm disc was punched. For the axial specimens a ring was cut with a diamond saw, then the ring was ground to a thickness of about 0.1 mm after which a length of arc of 3 mm was punched out from the ring.

The specimens were thinned to electron transparency by electropolishing them in a solution of 10% perchloric acid in ethanol at a temperature of about –26 °C.

2.3. Microscopy

The specimens were examined in a JEOL 2000 EX scanning transmission electron microscope at an acceleration voltage of 200 kV. Both examination work and chemical analysis were performed with the specimens in a conventional double-tilt holder. For the chemical microanalyses by energy dispersive spectroscopy (EDS) an Oxford Instruments Inca system was used. Pictures were recorded on conventional photographic film but after development the negatives were scanned to digital form in transmission mode in a flatbed scanner and saved to hard disk for subsequent treatment.

3. Results.

3.1. Irradiation induced microstructure

3.1.1 The plenum structure.

Figure 3 shows a typical example of the loop structure observed in the plenum specimen. The structure is characterized by a high density of loops, some of which appear as loops and some as black dots. There is a tendency for an alignment of the loops along a direction perpendicular to the row of systematic diffraction spots. There is a sibling picture to the one shown in Figure 3 in which the specimen has been tilted about 6° around the normal to the diffracting $(10\bar{1}1)$ plane in order to get a stereo pair. The diffraction pattern of that picture shows that the alignment is close the trace of the basal plane. The stereo pair in itself was used to ascertain that the observed black dots lie inside the foil and not on the surfaces. It also confirms that the linear objects seen in Figure 3 are short lengths of dislocations. It is interesting to speculate about the origin of these dislocations since recrystallized material does not normally contain many dislocations. Perhaps they are the result of creep down of the cladding under the 12 years of exposure in the reactor.

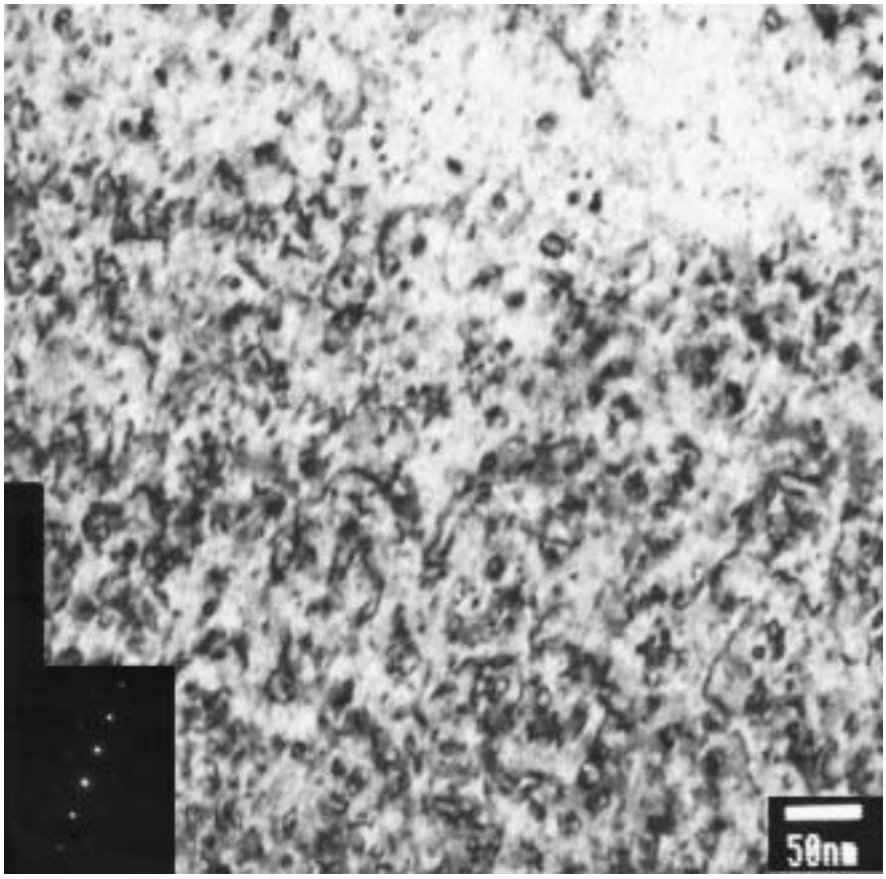

Figure 3. Loop structure observed in the plenum specimen. The inserted diffractogram shows the systematic $(10\bar{1}1)$ reflections. 200000x.

Figure 3 was taken on a radial specimen which means that the beam direction is approximately radial. In the examination of axial foils with the (0002) diffraction vector activated no dislocations could be seen. Thus there is no **c** component damage at the fluence and irradiation times characteristic of the plenum specimens.

The sizes of the clearly visible loops were measured. The sizes varied between 5 and 16 nm in diameter, with 11 nm as a mean value. The number density was determined to be 2.4×10^{22} m^{-3}. The value has been adjusted for the fact that one third of the loops are invisible in Figure 3 because of the $\mathbf{b} \cdot \mathbf{g} = 0$ invisibility criterion. In this calculation also loops visible as just black dots have been included. The foil thickness was not determined and a value of 100 nm was used. The values obtained for size and number density agree well with the results from the round-robin exercise of 1979 [5].

3.1.2 The low burnup structure.

The microstructure observed in the radial specimens shows a strong similarity to the

microstructure observed in the plenum specimen. A typical example is shown in Figure 4.

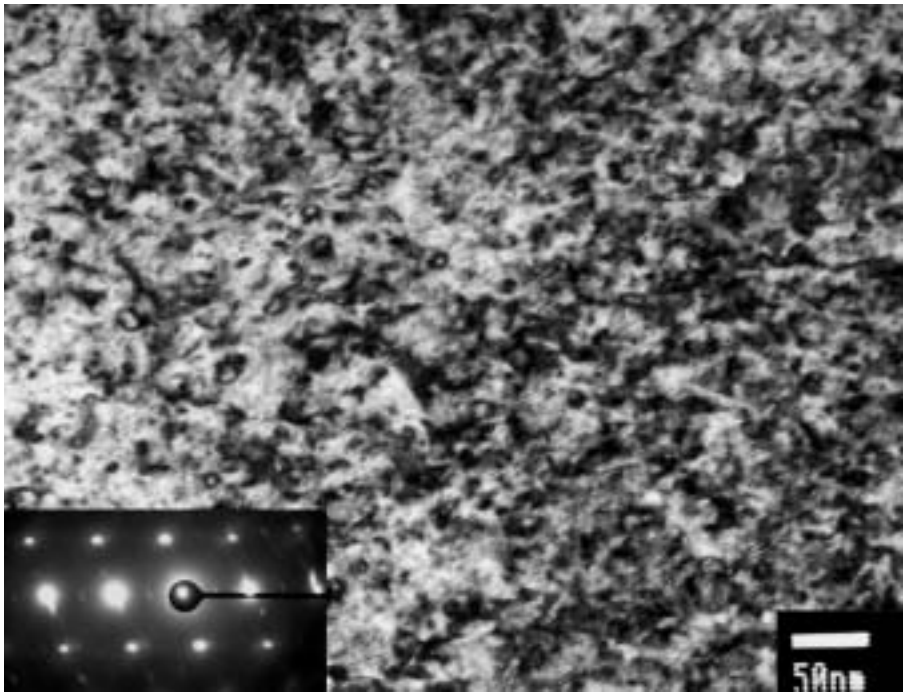

Figure 4. Loop structure observed in the low burnup specimen. The inserted diffractogram shows the systematic $(10\bar{1}1)$ reflections. 200000x.

An interesting structural feature found in the radial low burnup specimen is illustrated in Figure 5. It is a dark field picture taken with the spot at the arrow in the diffractogram in the centre of the objective aperture. At the time of taking the picture it was assumed that the spot represented diffraction from the surface hydride seen in the picture. However as can be seen in the picture a lot of small bright objects appeared in addition to the hydride. After tilting the specimen about 8° a new dark field picture was taken through the same spot. The same bright objects appeared and stereo viewing of the pictures revealed that they lie in the bulk of the foil. A puzzling circumstance is that the interplanar distance corresponding to the position of the spot is 0.20 nm which does not fit either of Zr matrix or hydride.

Figure 6 shows the **c** component damage in the low-burnup specimen. It seems to consist of short dislocation segments directed perpendicular to the c-axis of the material. The picture was taken with the (000x) row of systematic reflections activated. By tilting around the c-axis another picture was taken in order to get a stereo pair. The purpose of

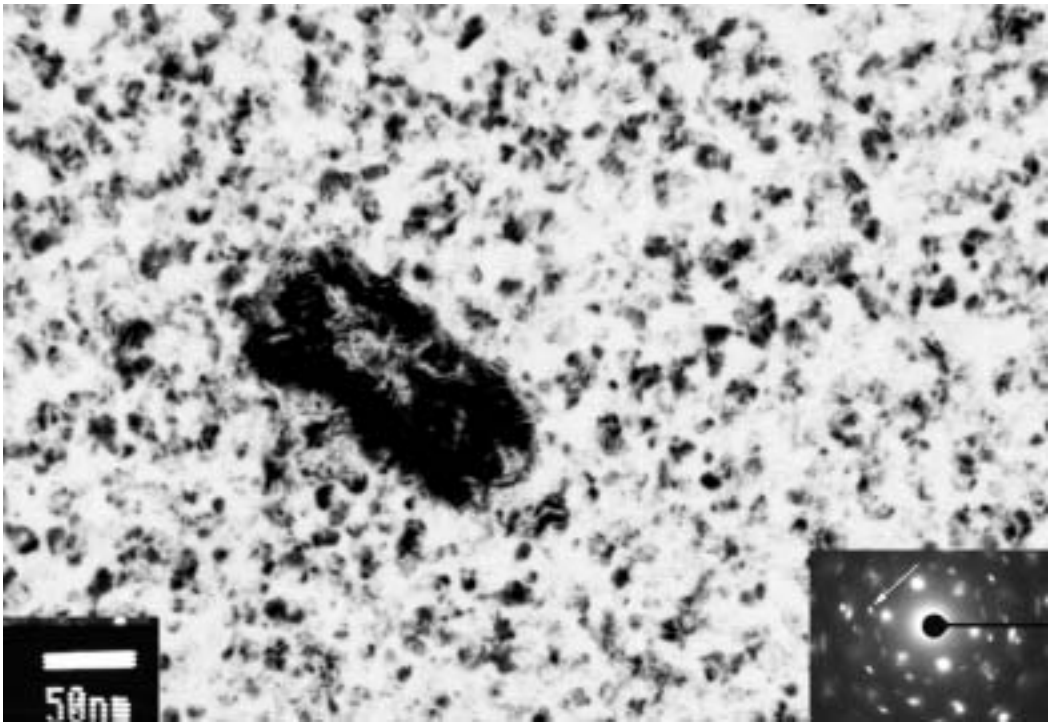

Figure 5. A surface hydride in the low burnup specimen. The black dots are an unidentified microstructural feature. The picture is a dark field picture which has been inverted in reproduction. 240000x.

of using stereo in this case was to see if the line segments go from the top of the foil to the bottom of the foil. However this did not seem to be the case so probably the segments are several small loops which when observed edge on appear as a segment.

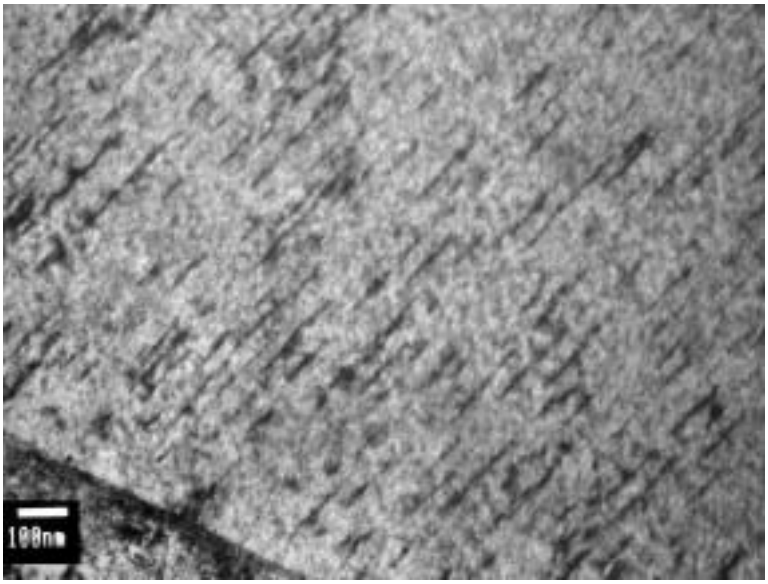

Figure 6. **c** component damage in the low burnup specimen. The c-axis is perpendicular to the direction of the apparent line segments. 65000x.

3.1.3 The high burnup structure.

In the radial specimen of the high burnup material it is very clear how the **a** component loops tend to align along the $<11\bar{2}0>$ direction, Figure 7. As can also be seen in Figure 7 the density of **a** type loops is so high that it is impossible to evaluate their size distribution and density.

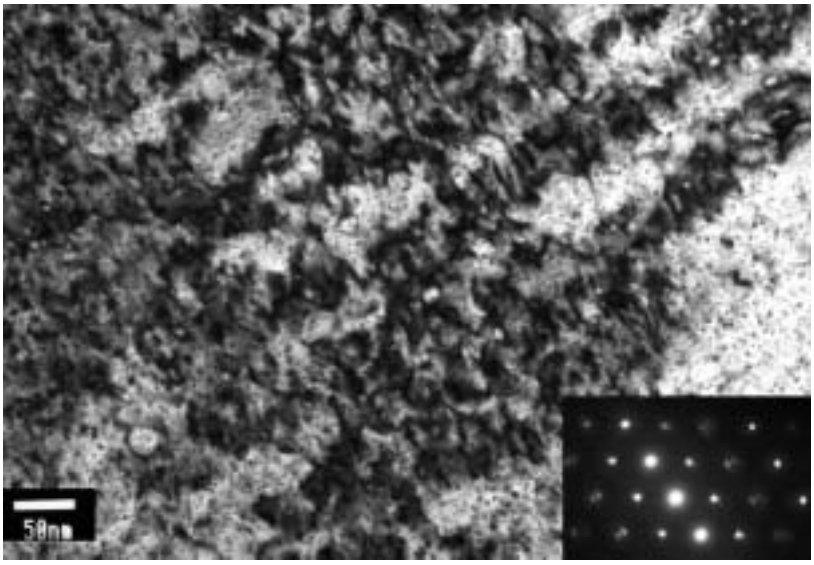

Figure 7. Alignment of **a** component loops along the $<11\bar{2}0>$ direction. 160000x.

As can be seen in Figure 8 the density of the **c** component damage is higher in the high burnup material than in the low burnup material.

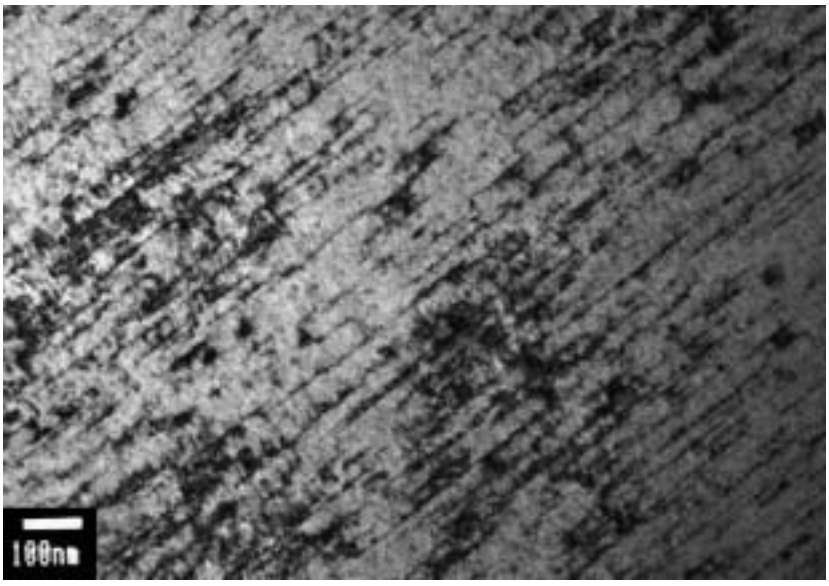

Figure 8. **c** component damage in the high burnup material. 80000x.

Figure 8 is also one of the pictures of a stereo pair which was used in order to better characterize the damage. The subjective impression from stereo viewing is that the the objects which look like short segments are in fact composed of linearly aligned smaller loops which are seen edge on.

3.2 Precipitates

3.2.1 The plenum sample

Figure 9 shows an example of particles observed in the plenum. The picture shows two particles and two elongated objects which probably are surface hydrides formed during electropolishing.

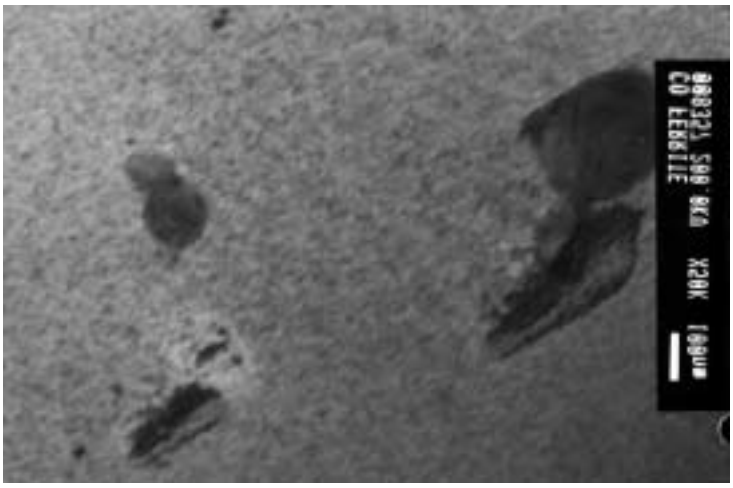

Figure 9. Two particles observed in the plenum sample. In the lower part of the picture two surface hydrides can be seen.

Energy dispersive X-ray analysis of the particles showed that the larger of the two particles contained Zr, Fe and Ni indicating that it is of the $Zr_2(Ni,Fe)$ type. The other particle contained Zr, Fe and Cr indicating that it is of the $Zr(Fe,Cr)_2$ type. This type of particle can have either a hexagonal or cubic crystal structure. The electron diffraction patterns indicated that the particles had the hexagonal structure. A number of chromium rich particles were analysed. The Cr/Fe-ratios measured varied from 1.5 to 3. In the only Ni rich particle analysed the ratio Ni/Fe was 1.3±0.2.

3.2.2 The low and high burnup samples

There was no obvious difference between particle numbers or sizes between the high burnup and low burnup samples. Most of the $Zr(Fe,Cr)_2$ particles were amorphous although an occasional crystalline particle could be found. Typical examples are shown in Figure 10.

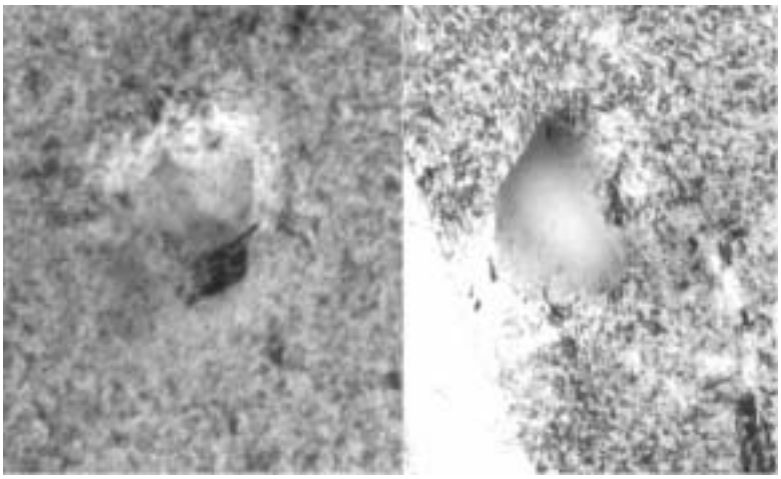

Figure 10. $Zr(Cr,Fe)_2$ type particles observed in the low burnup sample. The crystalline particle to the left represents an exception while most particles were amorphous like the particle to the right. 60000x.

EDS analyses showed an interesting difference between specimens with the radial and axial orientation. For the radial specimens the Cr/Fe ratio was generally greater than 20 while in the axial specimens Cr/Fe ~ 7-9. It is reasonable to interprete that observation as a result of anisotropic diffusion of Fe out of the particles. If the Fe tends to diffuse preferentially out from the particle along the basal plane some of the Fe which has left the particle may still be captured by the electron beam if it goes in the axial direction since the beam then goes along the basal plane.

Only one particle of the $Zr_2(Ni,Fe)$ type was observed. Analysis showed that it had the ratio Ni/Fe ~ 2.2, indicating that Fe tends to leave also this type of particle as a result of the irradiation.

3.3 Hydride structures

3.3.1 Unirradiated material.

In order to get some perspective on the observations on the irradiated material a sample of unirradiated material was examined. This sample came from a Zircaloy-2 tube which had been hydrided in a streaming mixture of 2.5% H_2 in argon for 3.5 h at 463 °C. At the location of the TEM specimen the hydrogen content was estimated to be 600-900 ppm. The TEM specimen was prepared from a metallographic cross section by cutting a thin ring from the metallographic mount and then proceeding as for the axial type specimens.

Diffraction patterns of the hydrides indicated that they were δ hydrides even though there is in most cases very difficult to differentiate between δ and γ hydrides. The orientation relationships were not determined except that a (111) reflexion of the hydride was always nearly coincident with the (0002) reflexion of the matrix. Generally there was a small angular deviation of about 1.5° between the close packed planes of hydride and matrix. These observations are consistent with the orientation relationships reported by Chung [24], that

$$(111)_{\delta\text{-hydride}} \,//\, (0001)_{\alpha-Zr}$$
$$[1\bar{1}0]_{\delta\text{-hydride}} \,//\, (1\bar{1}00)_{\alpha-Zr}$$

The habit plane was found to be consistent with other observations of $(10\bar{1}7)$ as the habit plane and well illustrated by the figure below.

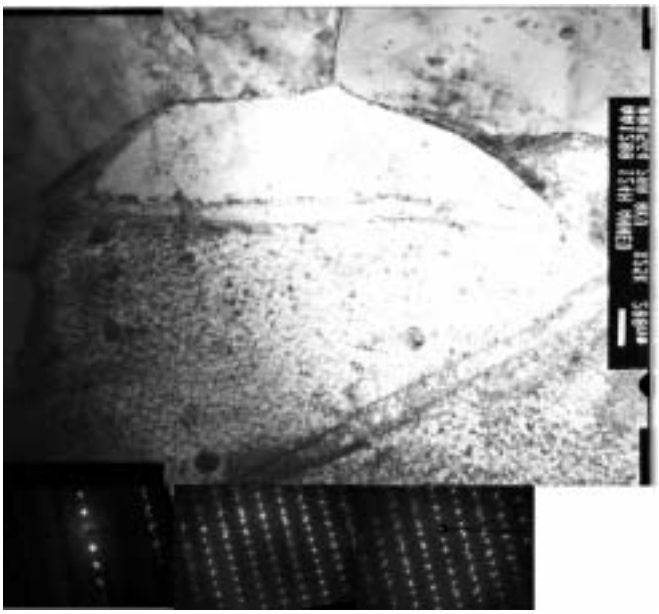

Figure 11. Two hydrides with different habit planes in one grain. The diffraction patterns show that the hydrides have the same crystallographic orientation relationship with the matrix. 10000x.

The basal plane lies perpendicular to the (000n) row of spots seen in the diffractograms and can be seen to bisect the angle between the two hydrides. Both hydrides make about a 76° angle with the basal plane which is consistent with the hydrides having a $(10\bar{1}7)$ habit plane. Although they have two different $(10\bar{1}7)$-planes as habit planes they have exactly the same crystallographic orientation.

3.3.2 Irradiated material.

Since there was no obvious difference between the hydride structures in the different irradiated samples the following account covers all three samples. Figure 12 illustrates a few typical features of the hydride structures observed in the irradiated samples.

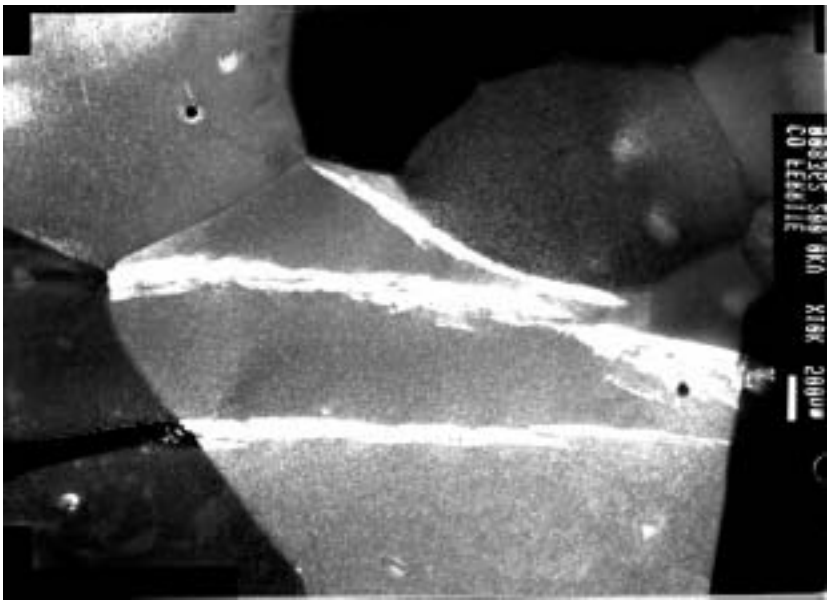

Figure 12. A dark field image of hydrides oberved in the low burnup specimen. 12000x.

The hydrides quite often appear several in parallel in the same grain. Up to four parallel hydrides have been observed. The picture also shows a hydride which follows a grain boundary, a feature also observed quite frequently. Where the two parallel hydrides meet the grain boundary two other hydrides begin in the adjacent grain. For the lower hydride in the Figure the hydride in the adjacent grain has been etched away and is not visible. Similar chains of hydrides going through up to four grains were observed in the specimens.

Another feature seen in Figure 12 is that the hydrides are somewhat irregular in shape and not quite continous. It is thus possible that the macroscopic hydrides actually are composed of smaller hydrides in agreement with Chung's proposal for the $(10\bar{1}7)$ habit plane for hydride precipitation [24]. According to Chung's proposal a macroscopic hydride is actually composed of several small hydrides with a (0002) habit plane which arrange themselves so that the collection of hydrides take on a $(10\bar{1}7)$ habit plane orientation.

However when a hydride is viewed in higher magnification there is nothing which indicates that it is composed of smaller hydrides, Figure 13. This hydride is rather typical of the hydrides observed in the irradiated material. It has a somewhat irregular shape with an internal microstructure which is difficult to resolve properly:

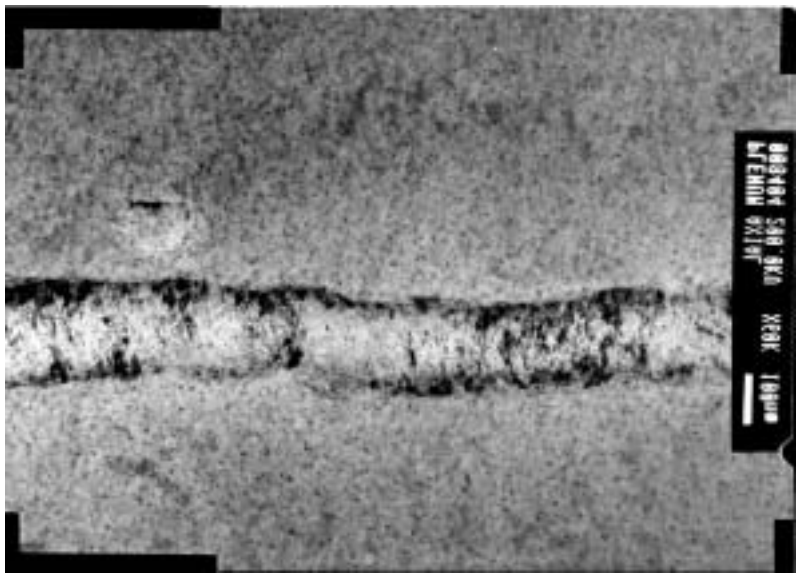

Figure 13. A hydride in the plenum sample. 70000x.

The internal structure in hydrides consist of dislocation segments which probably form in association with the precipitation of the hydride. It may be speculated that in addition to this initial internal structure there may also be a component due to the radiation damage. However attempts to unambiguously resolve any loop type damage in the hydrides were unsuccessful.

Crystallographically the habit plane of the hydrides seemed to be near $(10\bar{1}7)$ in the cases when it could be checked against the diffraction pattern. The orientation relationship with the matrix was such that the basal plane in the matrix was nearly parallel with a close-packed plane in the hydride. But there is always a slight misalignment of about 1.5°. Thus the hydrides in the irradiated materials behave similar to the hydrides in unirradiated material.

Chung observed a population of relatively small hydrides [26], which he thinks play a role in brittle fracture of spent cladding. Small hydrides were frequently observed in the present work. However it seems more reasonable to associate them with surface hydrides which form during specimen preparation [4]. Two examples are shown in Figure 9. In one other case a stereo pair was obtained which clearly indicated that the

hydride in question was located on the surface of the foil. The small hydrides observed in this work were not present in the majority of the grains, so even if they are bulk hydrides it is very unlikely that they play a significant role for the mechanical behaviour of this material.

4. Discussion.

The observations in the present investigation confirms previous studies of Zircaloy which has been irradiated to high neutron doses. At low doses as in the plenum sample the microstructure is dominated by **a** type loops which tend to be aligned along certain directions. In this work the $< 11\bar{2}0 >$ direction was noted in the case of the high burnup material where the alignment is more pronounced. The size distribution and density of **a** type loops tends towards saturation values which were apparently not reached in the plenum sample since the number densities appeared to be higher in the more irradiated samples.

At the higher doses the **c** component damage has started to be visible. This can previously been explained as a result of the beginning dissolution of second phase particles and the present observations are consistent with such an explanation. It appears as if the **c** component damage is slightly denser in the high burnup sample than in the low burnup sample. This is quite interesting in view of the large differences between the samples in terms of irradiation dose. So apparently there is a saturation effect for the **c** component damage in the same way as it is for the **a** type damage. Such a saturation is consistent with the nearly constant growth rate for recrystallized Zircaloy components at these dose. Basically one would expect the growth rate to be more or less proportional to the line length of **c** component dislocations. The slight upturn in growth rates deduced by Holt and Griffiths [15, 20] is consistent with the observed higher density of **c** type damage in the high burnup sample.

The micrstructural feature shown in Figure 5 is unfortunately not completely understood. It has a lower number density than the **a** type loops and it is illuminated in a dark field picture taken with a diffraction spot which does not fit either of matrix or hydride. Chung reported [21] a non-equilibrium precipitation of cubic ZrO_2 in irradiated Zircaloy but the diffraction spot used for the dark field image represents an interplanar spacing of 0.20 nm which does not fit cubic ZrO_2. One possibility is that the objects are reprecipitation of dissolved second phase particles. However if that is the case all precipitates have the same orientation since there would otherwise be diffraction rings from the particles. It seems unlikely that all particles should have the

same orientation, particularly in view of the fact that in another case of reprecipitation observed in a parallel investigation on the same material, the reprecipitated particles did have different orientations[28].

The observations on large hydrides confirmed Chung's determination of habit planes for delta hydrides in irradiated material. However no clear evidence was found which indicated that the large hydrides are composed of a collection of smaller hydrides each with a (0001) habit plane and only their collective perimeter following the $(10\bar{1}7)$ orientation. Another of Chung's observations not confirmed by the present investigation is the existence of a population of small delta hydrides. Small hydrides were observed, but not in every grain. And it is a reasonable assumption that these hydrides are the type of surface hydrides frequently formed during the electrolytic polishing of the specimens.

5. Conclusions.

The following conclusions have been drawn from the present investigation:

- Our observations are basically in agreement with previous studies of the microstructure of irradiated Zircaloy.

- Chung's observations of habit planes for hydrides in irradiated Zircaloy have been confirmed.

- The population of small hydrides observed by Chung is absent in the present material.

- Measured differences in the Cr/Fe ratio between radial and axial specimens confirm the anisotropy of diffusion in zirconium.

- There is nothing in the microstructure which might indicate that the material could be sensitive to fast brittle failure modes.

6. References.

1. Kelly, B.T., *Irradiation damage to solids*. First edition ed. 1966, Oxford: Pergamon Press Ltd. 232.

2. Bacon, D.J., *Point defects and clusters in the hcp metals: their role in the dose transition.* Journal of Nuclear Materials, 1993. **206**: p. 249-265.

3. Phythian, D.J.e.a., *A comparison of displacement cascades in copper and iron by melecular dynamics and its application to microstructural evolution.* Journal of Nuclear Materials, 1995. **223**: p. 245-261.

4. Griffiths, M., *A review of microstructure evolution in zirconium alloys during irradiation.* Journal of Nuclear Materials, 1988. **159**: p. 190-218.

5. Northwood, D.e.a., *Characterization of neutron irradiation damage in zirconium alloys - an international "round-robin" experiment.* Journal of Nuclear Materials, 1979. **79**: p. 379-394.

6. Northwood, D.A., Atomic Energy Review, 1976.

7. Holt, R.A., Gilbert, R. W., and Fidleris, V.. in *Effects of Radiation on Materials: Eleventh Symposium*. 1982: ASTM.

8. Tucker, R.P., Fidleris, V., and Adamson, R. B. *High-fluence irradiation growth of zirconium alloys at 644 to 725 K*. in *Zirconium in the Nuclear Industry: Sixth International Symposium.* 1982. Vancouver: ASTM.

9. Fidleris, V., Tucker, R. P., and Adamson, R. B. *An overview of microstructural factors that affect the irrdiation growth of zirconium alloys.* in *Zirconium in the Nuclear Industry: Seventh International Symposium.* 1987: ASTM.

10. Garzarolli, F., Dewes, P., Maussner, G., Basso, H.-H. *Effects of high neutron fluences on microstructure and growth of Zircaloy-4*. in *Zirconium in the Nuclear Industry: Eighth International Symposium*. 1988. San Diego: American Society for Testing and Materials.

11. Griffiths, M., Gilbert, R. W., *The formation of c-component defects in zirconium alloys during neutron irradiation.* Journal of Nuclear Materials, 1987. **150**: p. 169-181.

12. Griffiths, M., Gilbert, R. W., Fidleris, V. *Accelerated irradiation growth of zirconium alloys*. in *Zirconium in the Nuclear Industry: Eighth International Symposium*. 1988. San Diego: American Society for Testing and Materials.

13. Motta, A.T., Lefebvre, F., Lemaignan, C. *Amorphization of precipitates in Zircaloy under neutron and charged-particle irradiation*. in *Zirconium in the Nuclear Industry: Ninth International Symposium*. 1990. Kobe: American Society for Testing and Materials.

14. Gilbon, D., Simonot, C. *Effect of irradiation on the microstructure of Zircaloy-4*. in *Zirconium in the Nuclear Industry: Tenth International Symposium*. 1993. Baltimore: American Society for Testing and Materials.

15. Griffiths, M., Holt, R. A., Rogerson, A., *Microstructural aspects of accelerated deformation of Zircaloy nuclear reactor components during service.* Journal of Nuclear Materials, 1995. **225**: p. 245-258.

16. Nikulina, A.V.e.a. *Irradiation induced growth and microstructure evolution of Zr-1.2Sn-1Nb-0.4Fe under neutron irradiaton to high doses*. in *Effects of Radiation on Materials: 18th International Symposium*. 1997: American Society for Testing and Materials.

17. de Carlan, Y.e.a. *Influence of iron in the nucleation of <c> component dislocation loops in irradiated Zircaloy-4*. in *Zirconium in the Nuclear Industry: Eleventh International Symposium*. 1995. Garmisch-Partenkirchen: ASTM.

18. Shishov, V.N.e.a. *Influence of neutron irradiation on dislocation structure and phase composition of Zr-base alloys.* in *Zirconium in the Nuclear Industry: Eleventh International Symposium*. 1995. Garmisch-Partenkirchen: ASTM.

19. Griffiths, M., Mecke, J. F., Winegar, J. E. *Evolution of microstructure in Zr-alloys during irradiation*. in *Zirconium in the Nuclear Industry: Eleventh International Symposium*. 1995. Garmisch-Partenkirchen: ASTM.

20. Holt, R.A., et. al. *Non-linear irradiation growth of cold-worked Zircaloy-2*. in *Zirconium in the Nuclear Industry: Eleventh International Symposium*. 1995. Garmisch-Partenkirchen: ASTM.

21. Chung, H.M., Yaggee, F. L., Kassner, T. F. *Fracture behavior and microtructural characteristics of irradiated Zircaloy cladding.* in *Zirconium in the Nuclear Industry: Seventh International Symposium*. 1985. Strasbourg: American Society for Testing and Materials.

22. Efsing, P., Pettersson, K. *Delayed hydride cracking in irradiated Zircaloy cladding*. in *Zirconium in the Nuclear Industry: Twelth International Symposium*. 1998. Toronto: ASTM.

23. Edsinger, K., Davies, J. H., Adamson, R. B. *Degraded fuel cladding fractography and fracture behavior*. in *Zirconium in the Nuclear Industry: Twelth International Symposium*. 1998. Toronto: ASTM.

24. Chung, H.M., Daum, R. S., Hiller, J. M., Billone, M. C. *Characteristics fo hydride precipitation and reorientation in spent-fuel cladding*. in *Zirconium in the Nuclear Industry: Thirteenth International Symposium*. 2001. Annecy: American Society for Testing and Materials.

25. Westlake, D.G., *The habit planes of zirconium hydride in zirconium and Zircaloy.* Journal of Nuclear Materials, 1968. **26**: p. 208.

26. Chung, H.M. *Fundamental metallurgical aspects of axial splitting in Zircaloy cladding*. in *International Topical Meeting on Light Water Reactor Fuel Performance*. 2000. Park City: American Nuclear Society.

27. Lysell, G., *Information on Ringhals 1 "Two-Life rods", Private communication*. 2001.

28. Ohta, *Private communication*. 2001.